

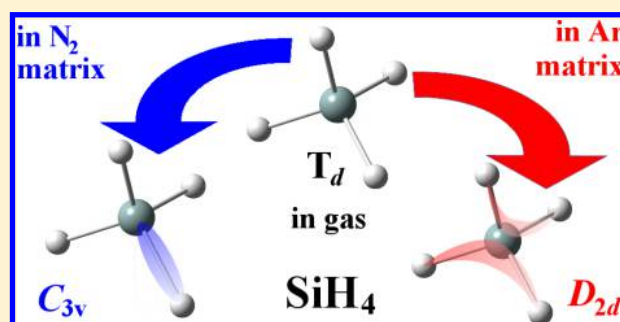
Infrared Studies of the Symmetry Changes of the $^{28}\text{SiH}_4$ Molecule in Low-Temperature Matrixes. Fundamental, Combination, and Overtone Transitions

Ruslan E. Asfin,¹ Tatjana D. Kolomiitsova, Dmitrii N. Shchepkin, and Konstantin G. Tokhadze*¹

Physical Faculty, St. Petersburg State University, 7/9 Universitetskaya Nab., 199034 Saint Petersburg, Russia

Supporting Information

ABSTRACT: Infrared spectra of $^{28}\text{SiH}_4$ in argon and nitrogen matrixes at low temperature 6.5–20 K in the region of overtone and combination transitions were recorded for the first time. Additionally, the high-resolution spectra were obtained in the fundamental region. The frequencies and the relative intensities of all bands were determined. The set of experimental data suggests that the symmetry of molecules studied in the matrixes is different from the symmetry of the free molecules because of an interaction with the environment. The symmetry of $^{28}\text{SiH}_4$ changes from T_d to C_{3v} on transition from the gas phase to a nitrogen matrix and to D_{2d} on transition to an argon matrix. A modeling of SiH_4 molecule force fields explains the experimental data as a change of a force constant of the selected SiH bond in the case of SiH_4 in the nitrogen matrix or force constants of two opposite angles in the case of SiH_4 in the argon matrix. In spite of small values of these changes, they result in noticeable spectroscopic effects: the band splitting and appearance of new bands in matrix spectra compared with spectra of free SiH_4 . The interpretation of transitions in the fundamental and combination regions was performed.



INTRODUCTION

The results of influence of low-temperature inert matrixes on the vibrational spectra of molecules are well-known. Inert matrixes slightly change the molecular systems, for most systems vibrational bands are narrowed, and their frequency and intensity change insignificantly.^{1–3}

For some systems the band splitting is observed, which is associated with the appearance of the so-called site structure. This splitting is explained by existence of different trapping centers in a matrix.² It should be mentioned that the appearance of additional bands and structure in the spectra can also be associated with the formation of weak van der Waals complexes, in particular, complexes characterized by resonant dipole–dipole (RDD) interactions. The formation probability of dimers, for example, $(\text{SF}_6)_2$,^{4–7} $(\text{SiF}_4)_2$,^{8,9} and others,⁴ increases at low temperatures $T < 10–15$ K.

In addition to these research directions in the inert matrixes, a promising direction of research appeared in the past decade that is associated with the study of changes in the symmetry of highly symmetric molecules in low-temperature inert matrixes.^{10–13} A noticeable influence of a nitrogen matrix on the absorption spectra of XH_4 molecules was established in previous works.^{12,13} It was shown that the absorption spectra of silane and germane are similar in the regions of the stretching ν_3 and bending ν_4 vibrations. Moreover, for $^{28}\text{SiH}_4$ and $^{76}\text{GeH}_4$ in a nitrogen matrix, a triplet is observed in the stretching region and a doublet in the bending region,¹³ which

is explained by the change of the symmetry of an XH_4 molecule from T_d in the gas phase to C_{3v} in solid nitrogen.

In this article we continue the study of the changes in the symmetry of some symmetric molecules, in low-temperature matrixes. To increase the efficiency of the analysis of possible splitting of spectral bands, we recorded the high-resolution, up to 0.01 cm^{-1} , spectra. The second important feature of the intended experiment is to obtain spectra in the overtone and combination band range. Investigation of spectra in the overtone and combination regions allows studying the anharmonicity effects when the symmetry of molecules or complexes changes. It should be noted that the spectra in these regions in low temperature matrixes are rarely discussed in the literature.^{14–23} The advantage of these investigations is that the spectral changes (shifts and splitting) are more pronounced in comparison with transformations of the spectra in the fundamental region because of higher sensitivity of overtones and combination transitions to external perturbation. Analysis of the band transformations in the overtone region will provide a final interpretation of the observed spectral changes.

With regard to the objects of research, for registration of high-resolution spectra it is advisable to use monoisotopic $^{28}\text{SiH}_4$. The highly symmetric SiH_4 molecule is a popular object

Received: March 24, 2017

Revised: June 19, 2017

Published: June 20, 2017

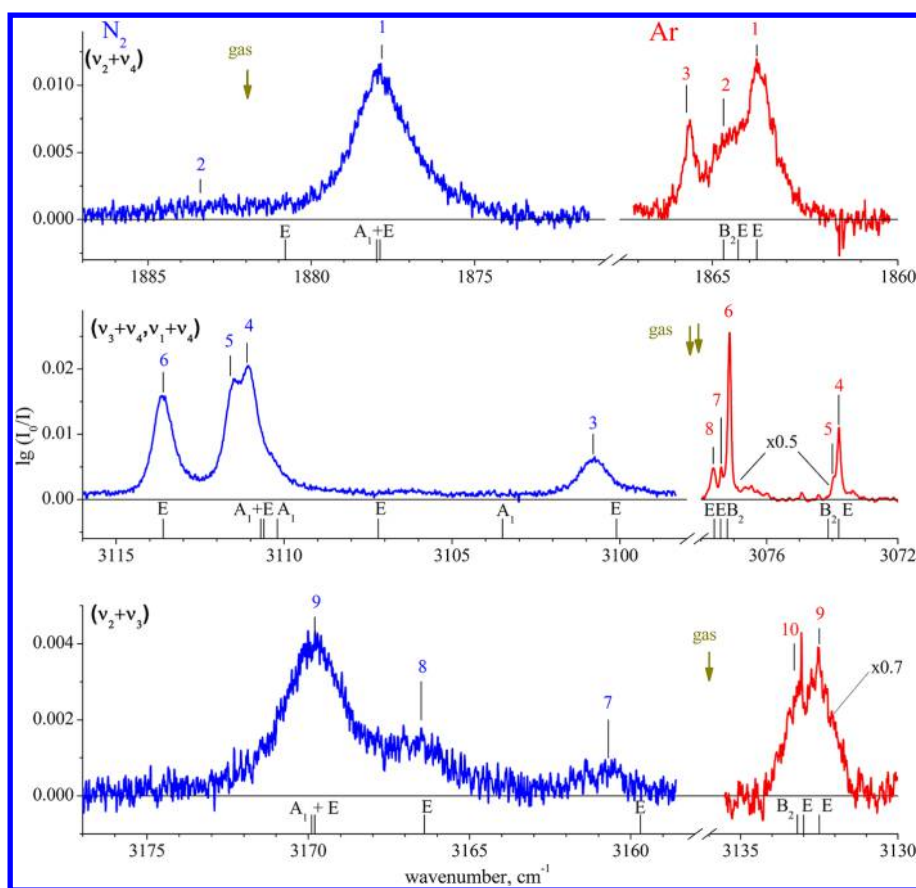


Figure 1. Spectra of $^{28}\text{SiH}_4$ in the $(\nu_2 + \nu_4)$ (top panel), $(\nu_3 + \nu_4, \nu_1 + \nu_4)$ (middle panel), and $(\nu_2 + \nu_3)$ (bottom panel) regions in nitrogen (left spectra) and argon (right spectra) matrixes at $T = 6.7$ K. The spectra were obtained by deposition at $T = 15$ K of mixtures of initial concentrations: $\text{SiH}_4/\text{N}_2 = 1/1000$ and $\text{SiH}_4/\text{Ar} = 1/550$. The i th spectral components from Tables 1 and 2 are marked by numbers. The arrows indicate positions of the gas phase transitions in the corresponding regions (1881.96 cm^{-1} in $(\nu_2 + \nu_4)$,³¹ 3095.26 and 3098.02 cm^{-1} in $(\nu_3 + \nu_4, \nu_1 + \nu_4)$,³⁶ and 3152.59 cm^{-1} in $(\nu_2 + \nu_3)$ ³⁶). Between the spectra in nitrogen and argon matrixes, there are gaps in the frequency scale. Vertical lines under the spectra indicate the frequencies of transitions with the corresponding symmetry species, which are calculated using the simplest model (see text for details).

of study of the influence of intermolecular interactions on the spectral and structural characteristics of cryogenic systems.^{24–27}

Its principal advantages are as follows: it is a relatively simple and small (in comparison with the “heavy” molecules SF_6 , SiF_4 , CF_4 , etc.) molecule, which does not rotate^{24,27} in low-temperature matrixes (in contrast to CH_4 ^{28,29}), and due to large amplitudes of vibrations, this molecule is very sensitive to the influence of its surroundings. The high intensities of the triply degenerate ν_3 stretching ($A_3 = 282\text{ km/mol}$) and ν_4 bending ($A_4 = 381\text{ km/mol}$) absorption bands are very useful in the experimental measurement of the absorption spectra of SiH_4 in different conditions.

The purpose of this article is to study the fine structure of the vibrational spectra of monoisotopic $^{28}\text{SiH}_4$ molecule in low temperature nitrogen and argon matrixes in the $5500\text{--}600\text{ cm}^{-1}$ spectral range. The high-resolution spectra of SiH_4 were recorded at a temperature of $6.5\text{--}20\text{ K}$ with a resolution of $0.01\text{--}0.1\text{ cm}^{-1}$. The frequencies and the relative intensities of all bands were determined. The main goal is to record spectra in the region of overtones and combination bands. For comparison, we recorded also the spectra in the fundamental range (in the regions of ν_3 stretching and ν_4 bending vibrations) with higher resolution than it has been done before.

EXPERIMENTAL SECTION

The standard manometric technique was used for pumping system and preparation of gas mixtures. Gas mixtures of SiH_4 with Ar and N_2 were prepared by adding argon or nitrogen into a 2 L stainless steel bulb containing $^{28}\text{SiH}_4$ at an initial pressure of $p = 0.8\text{--}2.5\text{ mbar}$, so the initial concentration of the gaseous mixtures SiH_4/Ar (N_2) was between 1:300 and 1:1000. To obtain a lower concentration of SiH_4 (down to 1:10000), the mixture was pumped out to pressure $100\text{--}250\text{ mbar}$ and diluted by matrix gas (Ar or N_2) to a desirable ratio. The pressures under 100 mbar were measured with a MKS Baratron capacitance manometer (upper limit 100 mbar , accuracy 0.25% of reading); the higher pressures were measured with a Swagelok gauge (range, $1\text{--}0.6\text{ bar}$; accuracy class 1.0).

The gas mixtures of $^{28}\text{SiH}_4$ with N_2 or Ar were deposited on a gold-plated copper mirror at a temperature $10\text{--}20\text{ K}$. The temperature of the mirror placed in the vacuum unit was maintained by a closed cycle helium cryostat (Sumitomo Cold Head model CH-204 equipped with a Cryocon Model 32 temperature controller). The temperature was measured with diode sensors. We estimate the absolute error in temperature to be no more than 0.2 K . The deposition was monitored by the infrared spectrum of the matrix. The deposition rate was controlled by low-flow metering valve, the deposition time changed from 5 min to 6 h. The matrixes were annealed during $15\text{--}30\text{ min}$ at a temperature of $25\text{--}32\text{ K}$. The spectra were

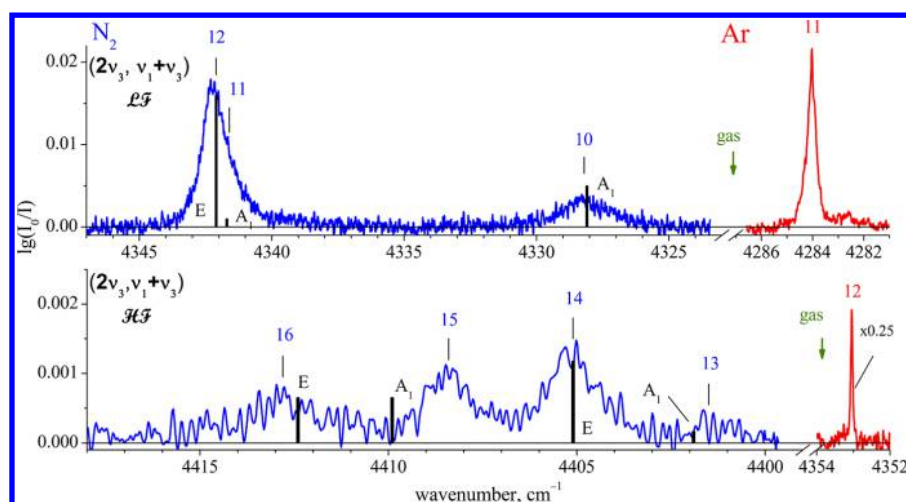


Figure 2. Spectra of $^{28}\text{SiH}_4$ in the $(2\nu_3, \nu_1 + \nu_3)$ Darling–Dennison resonance region near the low-frequency component (top panel) and near the high-frequency component (bottom panel) in nitrogen (left spectra) and argon (right spectra) matrixes at $T = 6.7$ K. The spectra were obtained by deposition at $T = 15$ K of mixtures of initial concentrations: $\text{SiH}_4/\text{N}_2 = 1/1000$ and $\text{SiH}_4/\text{Ar} = 1/550$. The i th spectral components from Tables 1 and 2 are marked by numbers. The arrows indicate positions of the gas phase transitions of corresponding components (4309.35 and 4380.28 cm^{-1}).³⁵ Between spectra in nitrogen and argon matrixes, there are gaps in the frequency scale. For comparison, the calculated stick spectrum (bold lines) and the symmetry species of the corresponding components are shown (see text for details).

Table 1. Characteristics of Splitting Components (i) of Absorption Combination Bands of $^{28}\text{SiH}_4$ (Frequencies ($\nu_{\text{N}_2}^i$, cm^{-1}), Shifts Relative to the Gas Phase Bands ($\Delta\nu$,^a cm^{-1}), Full Widths (fwhm, cm^{-1}), Intensities (I_i , (%)), and Relative Intensities I rel = $1000(\sum I_i)/I(\nu_3)$) in the N_2 Matrix at $T = 6.7(2)$ K

| spectral range | i | $\nu_{\text{N}_2}^i$, cm^{-1} | $\Delta\nu$, ^a cm^{-1} | fwhm, cm^{-1} | $I_i/(\sum I_i)$, % | I rel | symmetry species ^b |
|--|----|---|---|------------------------|----------------------|---------|-------------------------------|
| $(\nu_2 + \nu_4)$ | 1 | 1877.8 | −4.2 | 2.1 | 90(5) | 5.8(5) | ($A_1 + E$) |
| | 2 | 1883.4 | +1.4 | 4.6 | 10(5) | | (E) |
| $(\nu_1 + \nu_4)$ | 3 | 3100.8 | +5.5 | 0.8 | 16(1) | 9.3(4) | (E) |
| | 4 | 3111.1 | +13.1 | 0.7 | 42(4) | | (A_1) |
| $\nu_3 + \nu_4$ | 5 | 3111.6 | +13.6 | 0.4 | 14(2) | | ($A_1 + E$) |
| | 6 | 3113.6 | +15.6 | 0.6 | 28(3) | | (E) |
| $(\nu_2 + \nu_3)$ | 7 | 3160.7 | +8.1 | 1.7 | 11(1) | 3.5(2) | (E) |
| | 8 | 3166.5 | +13.9 | 2.2 | 25(3) | | (E) |
| | 9 | 3169.8 | +17.2 | 2.2 | 65(5) | | ($A_1 + E$) |
| $(2\nu_3, \nu_1 + \nu_3)$ \mathcal{LF} | 10 | 4328.2 | +18.8 | 2.6 | 24(2) | 8.3(1) | (A_1) |
| | 11 | 4341.6 | +32.2 | 0.9 | 15(5) | | (A_1) |
| | 12 | 4342.1 | +32.7 | 0.7 | 61(5) | | (E) |
| $(2\nu_3, \nu_1 + \nu_3)$ \mathcal{HF} | 13 | 4401.5 | +21.2 | 0.7 | 7(4) | 0.22(2) | (A_1) |
| | 14 | 4405.1 | +24.8 | 0.8 | 40(5) | | (E) |
| | 15 | 4408.4 | +28.1 | 0.7 | 26(3) | | (A_1) |
| | 16 | 4412.8 | +32.5 | 1.2 | 27(3) | | (E) |

^a $\Delta\nu = \nu_{\text{N}_2}^i - \nu^{\text{gas}}$; $(\nu_2 + \nu_4)^{\text{gas}} = 1881.96$ cm^{-1} ,³¹ $(\nu_3 + \nu_4, \nu_1 + \nu_4)^{\text{gas}} = 3095.26$ and 3098.02 cm^{-1} ,³⁶ $(\nu_2 + \nu_3)^{\text{gas}} = 3152.59$ cm^{-1} ,³⁶ and $(2\nu_3, \nu_1 + \nu_3)^{\text{gas}} = 4309.35$ and 4380.28 cm^{-1} .³⁵ ^bMolecular symmetry is C_{3v} in N_2 matrixes.

measured in the temperature interval $T = 6.5$ – 20 K before and after annealing.

The spectra were recorded with a Bruker 125HR Fourier-spectrometer equipped with a Ge/KBr beam splitter with a resolution of 0.01 – 0.1 cm^{-1} . A LN-MCT detector was used for recording spectra in 4500 – 600 cm^{-1} range, and a LN-InSb detector was used to obtain spectra in 5500 – 1850 cm^{-1} range. Each spectrum was obtained by averaging 100 interferograms and using the Norton–Beer medium apodization function. Low-temperature cryostat with KBr window was mounted outside the vacuum Fourier spectrometer with special optical system Bruker A515/1.

The monoisotopic sample of $^{28}\text{SiH}_4$ (99.99% of ^{28}Si) was obtained from the Institute of Chemistry of High Purity

Substances of the Russian Academy of Sciences. We used Ar and N_2 with a purity of 99.99%

RESULTS

The spectra of SiH_4 in the region of combination transitions have been measured in low temperature matrixes for the first time. High-resolution spectra allowed us to obtain new information about the band splitting. In the figures and tables that present the results of the matrix measurements in the region of combination and fundamental transitions we used the same notations of vibrational transitions as in the gas phase where SiH_4 molecules have the T_d symmetry.

The spectra of $^{28}\text{SiH}_4$ in N_2 and Ar matrixes in the region of combination bands with $\text{SiH}_4/\text{M} = 1/(500$ – $1500)$, where $\text{M} = \text{N}_2$ and Ar, are shown on the same frequency scale in Figures 1

Table 2. Characteristics of Splitting Components (i) of Absorption Combination Bands of $^{28}\text{SiH}_4$ (Frequencies (ν_{Ar}^i , cm^{-1}), Shifts Relative to the Gas Phase Bands ($\Delta\nu$, cm^{-1}), Full Widths (fwhm, cm^{-1}), Intensities (I_i (%)), and Relative Intensities $I \text{ rel} = 1000(\sum I_i)/I(\nu_3)$ in the Ar Matrix at $T = 6.7(2)$ K; the Frequencies, Shifts, and Relative Intensities of the Combination Bands in the Liquid Argon (LAr) are Given for Comparison³⁰

| spectral range | i | ν_{Ar}^i , cm^{-1} | $\Delta\nu$, ^a cm^{-1} | fwhm, cm^{-1} | $I_i/(\sum I_i)$, % | $I \text{ rel}$ | symmetry species ^b | LAr | |
|----------------------------------|----|--|---|------------------------|----------------------|-----------------|-------------------------------|--|-----------------|
| | | | | | | | | ν , $\text{cm}^{-1}/\Delta\nu$, ^a cm^{-1} | $I \text{ rel}$ |
| $(\nu_2 + \nu_4)$ | 1 | 1863.8 | -18.2 | 0.9 | 51(3) | 6.1(5) | (E) | 1871/ | 8.8 |
| | 2 | 1864.7 | -17.3 | 1.1 | 36(2) | | (E) | -11 | |
| | 3 | 1865.7 | -16.3 | 0.3 | 13(2) | | (B ₂) | | |
| $(\nu_1 + \nu_4, \nu_3 + \nu_4)$ | 4 | 3074.0 | -21.3 | 0.12 | 17(1) | 11.5(5) | (E) | 3089/ | 11 |
| | 5 | 3074.2 | -21.1 | 0.09 | 13(1) | | (B ₂) | -8 | |
| | 6 | 3077.4 | -20.6 | 0.10 | 40(2) | | (B ₂) | | |
| | 7 | 3077.6 | -20.4 | 0.08 | 6(3) | | (E) | | |
| | 8 | 3077.8 | -20.2 | 0.15 | 24(2) | | (E) | | |
| $(\nu_2 + \nu_3)$ | 9 | 3132.5 | -20.1 | 0.6 | 48(5) | 4.5(5) | (E) | 3147/ | 5.1 |
| | 10 | 3133.3 | -19.3 | 0.75 | 52(5) | | (B ₂ + E) | -6 | |
| $(2\nu_3, \nu_1 + \nu_3)$ | 11 | 4284.3 | -25.1 | 0.45 | 100 | 7.6(5) | (B ₂ + E) | 4304/ | 6.8 |
| | 12 | 4353.3 | -27.0 | 0.2 | 100 | 0.5(2) | (B ₂ + E) | -5 | |
| | | | | | | | | 4373/ | 0.32 |
| | | | | | | | | -7 | |

^a $\Delta\nu = \nu_{\text{Ar}}^i - \nu^{\text{gas}}$, the values of ν^{gas} in different regions. See footnote to Table 1. ^bMolecular symmetry is D_{2d} for SiH_4 in Ar matrixes.

and 2. The combination bands in the low-temperature matrixes are split into a number of components. These components are marked by numbers 1 to 16 in nitrogen matrixes and by numbers 1 to 12 in argon matrixes. The position of the combination bands in the regions $(\nu_2 + \nu_4)$, $(\nu_3 + \nu_4, \nu_1 + \nu_4)$, $(\nu_2 + \nu_3)$, and $(2\nu_3, \nu_1 + \nu_3)$ in the gas phase in these figures are indicated by arrows. Tables 1 and 2 present information on the frequencies, half-widths, and relative intensities of all splitting components (i) of the studied bands at $T = 6.7(2)$ K. The data of several experiments were averaged, the error was mainly determined by the temperature dependence of measured spectral parameters. For comparison, information on the characteristics of bands of SiH_4 in a solution in liquid argon³⁰ at $T = 90$ K, where the number of observed bands does not differ from the gas phase, is also presented in Table 2.

The intensities of bands in the region of combination bands are low, particularly in the case of dilute mixtures ($\text{SiH}_4/\text{M} = 1/(500-1000)$, when $I_0/I < 0.01$), and to make recording of the absorption bands reliable, the prepared mixtures were deposited onto a cold mirror within a few hours. In the $(2\nu_3, \nu_1 + \nu_3)$ region, where the optical density is less than 0.002, the deposition time reached 5–6 h.

The spectra recorded in N_2 matrixes differ essentially from the spectra recorded in Ar matrixes. One can see that in the Ar matrixes all SiH_4 bands are shifted, as usual, toward lower frequencies, with respect to the gas phase, but in the nitrogen matrixes the combination bands are blue-shifted. The exception is the bending region $(\nu_2 + \nu_4)$ where a small red shift of the splitting components is observed in the nitrogen matrix.

As for the fundamental transitions, the spectra of SiH_4 in the regions of the ν_1 and ν_3 stretching and ν_4 bending vibrations are not qualitatively different from the spectra recorded by us earlier^{12,13} with a resolution of $0.1-0.2 \text{ cm}^{-1}$; however, the high-resolution spectra allowed us to measure the splitting values of bending and stretching vibrations. Spectra in the region of the ν_3 stretching and ν_4 bending vibrations of $^{28}\text{SiH}_4$ in N_2 and Ar matrixes ($\text{SiH}_4/\text{M} = 1/(5000-10000)$, where $\text{M} = \text{N}_2, \text{Ar}$) are shown, in Figure 3. The spectral characteristics (the frequencies, half-widths, and relative intensities) of i th splitting components of these bands are listed in Table 3.

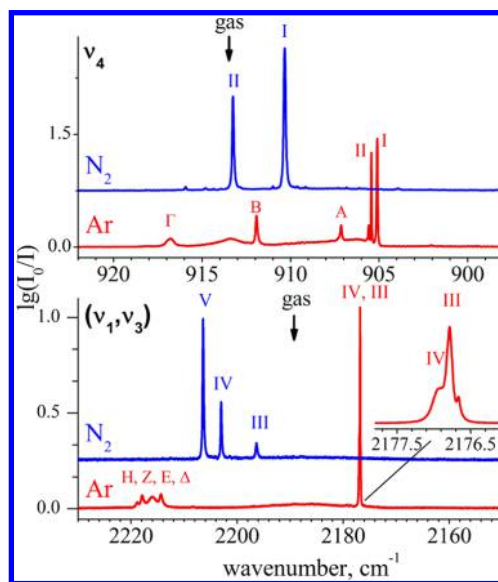


Figure 3. Spectra of $^{28}\text{SiH}_4$ in the ν_4 (top panel) and ν_3 (bottom panel) regions in nitrogen (top spectra) and argon (bottom spectra) matrixes at $T = 6.7$ K. The spectra were obtained by deposition of mixtures of concentration $\text{SiH}_4/\text{N}_2 = 1/6000$ (at 10 K) and $\text{SiH}_4/\text{Ar} = 1/10000$ (at 15 K). The arrows indicate positions of the gas phase transitions ($\nu_4 = 913.47$, $\nu_3 = 2189.19 \text{ cm}^{-1}$).³¹ The Roman numerals mark the i th bands from Table 3. The capital Greek letters denote the i th bands from Table 4 (for Ar matrixes). The inset shows the high-resolution spectrum of the ν_3 band in the $2177.8-2176.0 \text{ cm}^{-1}$ region.

Positions of the ν_3 and ν_4 bands in the gas phase spectra in this figure are indicated by arrows. In nitrogen and argon matrixes these components are marked with Roman numerals from I to V. The high-resolution spectra allow us to reliably measure the half-width of spectral components, which equal $0.1-0.3 \text{ cm}^{-1}$ in the nitrogen matrixes and reach 0.03 cm^{-1} in argon matrixes, see Table 3.

The most simple vibrational spectra of SiH_4 are observed in nitrogen matrixes, where only narrow components are recorded, two in the region of the ν_4 vibrations, marked by

Table 3. Characteristics of Splitting Components (i) in the Stretching (ν_3, ν_1) and Bending (ν_4) Spectral Regions of $^{28}\text{SiH}_4$ (Frequencies (ν_{M}^i , cm^{-1}), Shifts Relative to the Gas Phase Bands ($\Delta\nu$, cm^{-1}), Full Widths (fwhm, cm^{-1}), Intensities (I_i (%)), and Relative Intensities $I \text{ rel} = 1000(\sum I_i)/I(\nu_3)$ in the N_2 and Ar matrixes at $T = 6.7 \text{ K}$

| matrix | spectral range | i | ν_{M}^i , cm^{-1} | $\Delta\nu$, cm^{-1} | fwhm, cm^{-1} | $I_i/(\sum I_i)$, % | symmetry species ^c | I_{rel} |
|--------------|----------------|-----|---------------------------------------|--------------------------------|------------------------|----------------------|-------------------------------|------------------|
| N_2 | ν_4 | I | 910.34 | -3.1 | 0.12 | 65 | (E) | 1400 |
| | | II | 913.25 | -0.2 | 0.11 | 35 | (A ₁) | |
| | | III | 2196.33 | +7.1 | 0.35 | 10 | (A ₁) | |
| | ν_3, ν_1 | IV | 2203.00 | +13.8 | 0.22 | 24.5 | (A ₁) | 1000 |
| | | V | 2206.40 | +17.2 | 0.24 | 65.5 | (E) | |
| Ar | ν_4 | I | 905.11 | -8.3 | 0.06 | 70 | (E) | 1200 |
| | | II | 905.44 | -8.0 | 0.03 | 30 | (B ₂) | |
| | ν_3, ν_1 | III | 2176.79 | -12.4 | 0.09 | 67 | (E) | 1000 |
| | | IV | 2176.95 | -12.6 | 0.17 | 33 | (B ₂) | |

^a $\text{M} = \text{N}_2$ for N_2 matrix frequencies and $\text{M} = \text{Ar}$ for Ar matrix frequencies. ^b $\Delta\nu = \nu_{\text{M}}^i - \nu_{\text{gas}}^i$; $\nu_4^{\text{gas}} = 913.4 \text{ cm}^{-1}$, $\nu_3^{\text{gas}} = 2189.2 \text{ cm}^{-1}$. ^cMolecular symmetry is D_{2d} for SiH_4 in Ar matrixes and C_{3v} in N_2 matrixes.

numerals (I, II), and three in the ν_3 region, marked by (III, IV, V), respectively, see Figure 3. In the ν_3 stretching region the narrow bands are blue-shifted relative to the gas phase $\Delta\nu_3 = \nu_3^{\text{N}_2} - \nu_3^{\text{gas}} > 0$ ($\nu_3^{\text{gas}} = 2189.2 \text{ cm}^{-1}$), where, $\Delta\nu_3 = +7.1, +13.8$, and $+17.2 \text{ cm}^{-1}$ for III, IV, and V components, respectively. In the ν_4 bending region the center of gravity of two narrow bands is shifted slightly to lower frequencies relative to the gas phase frequency $\nu_4^{\text{gas}} = 913.4 \text{ cm}^{-1}$, here $\Delta\nu_4 = -3.1, -0.2 \text{ cm}^{-1}$ for components I and II, respectively. The ratios of intensities of splitting components I–V practically do not depend on the deposition conditions and annealing temperatures.

The spectra recorded in argon matrixes are complex and differ significantly from the SiH_4 spectra in nitrogen matrixes. In the ν_4 bending region a doublet with narrow components I and II and a splitting $\delta\nu_4 \approx 0.3 \text{ cm}^{-1}$ is observed. The inset in Figure 3 shows the high-resolution spectrum of the narrow ν_3 band in the region of $2177.8\text{--}2176.0 \text{ cm}^{-1}$. By using the standard procedures with the Lorentzian contours, this band can be separated into two main components with the frequencies 2176.79 and 2176.95 cm^{-1} . The Lorentzian contours allowed the experimental spectra to be described satisfactorily. In Ar matrixes the narrow bands in the bending and stretching regions are shifted, as usual, toward lower frequencies, $\Delta\nu_k = \nu_k^{\text{Ar}} - \nu_k^{\text{gas}} < 0$, so $\Delta\nu_4 \approx -8.1 \text{ cm}^{-1}$, $\Delta\nu_3 \approx -12.3 \text{ cm}^{-1}$.

The principal feature of the spectra of SiH_4 in argon matrixes is that, in addition to the narrow components, a number of wider blue-shifted bands are always recorded under these conditions. The relative intensities of these bands to narrow components in the ν_3 and ν_4 regions noticeably depend on the deposition and annealing temperatures. In the ν_4 region three bands marked with letters A, B, and Γ are observed, see Figure 3 and Table 4. One can see in Figure 3 that in the stretching region the broad band is blue-shifted from ν_3^{gas} by $20\text{--}25 \text{ cm}^{-1}$. This broad absorption in the spectra after annealing can be separated into four components, indicated by letters Δ , E, Z, and H (see Figures 3 and 4), and the spectral parameters of these bands are presented in Table 4. It should be noted that a similar absorption is observed in the combination ($2\nu_3, \nu_1 + \nu_3$) region (see Figure 4). The weak broad absorption, which includes four components, indicated by η , ζ , ϵ , and δ , is recorded on the high frequency side of the narrow component of the ($2\nu_3, \nu_1 + \nu_3$) band, which is indicated by the number 12 (see Table 2).

In addition to the marked bands, several weak bands (in particular, $913.5, 905.59$, and 2176.95 cm^{-1}) are present in the

Table 4. Characteristics of Bands (i) of Low Symmetry Molecules in the Stretching (ν_3, ν_1), Bending (ν_4), and Overtone ($2\nu_3, \nu_1 + \nu_3$) Spectral Regions of $^{28}\text{SiH}_4$ (Frequencies (ν_{Ar}^i , cm^{-1}), Full Widths (fwhm, cm^{-1}), Intensities (I_i (%)), and Relative Intensities $I \text{ rel} = 1000(\sum I_i)/I(\nu_3)$ in Ar matrixes at $T = 6.7 \text{ K}$

| spectral range | i | ν_{Ar}^i , cm^{-1} | fwhm, cm^{-1} | $I_i/(\sum I_i)$, % | $I \text{ rel}$ |
|---------------------------|------------|--|------------------------|----------------------|-----------------|
| ν_4 | A | 907.2 | 0.1 | 24 (2) | 1200 |
| | B | 911.9 | 0.1 | 40 (3) | |
| | Γ | 916.8 | 0.4 | 36 (2) | |
| ν_3 | Δ | 2214.4 | 0.7 | 22 (2) | 1000 |
| | E | 2216.0 | 1.7 | 54 (3) | |
| | Z | 2217.9 | 0.6 | 18 (2) | |
| | H | 2218.9 | 0.4 | 6 (2) | |
| $(2\nu_3, \nu_1 + \nu_3)$ | δ | 4358.1 | 3.1 | 31 (4) | ~ 10 |
| | ϵ | 4360.9 | 2.7 | 13 (4) | |
| | ζ | 4363.8 | 4.8 | 31 (4) | |
| | η | 4367.6 | 2.6 | 25 (4) | |

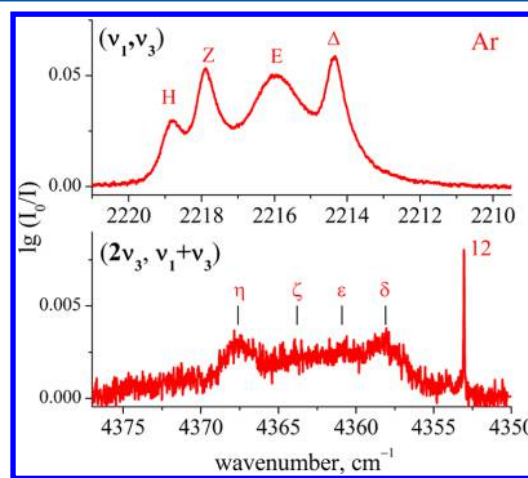


Figure 4. Spectra of low symmetry $^{28}\text{SiH}_4$ molecules in argon matrix at $T = 6.7 \text{ K}$ in the ν_3 (top panel) and ($2\nu_3, \nu_1 + \nu_3$) regions. The spectra were obtained by deposition at $T = 15 \text{ K}$ of mixtures of initial concentrations: $\text{SiH}_4/\text{Ar} = 1:1000$ in the fundamental region and $\text{SiH}_4/\text{Ar} = 1:550$ in the ($2\nu_3, \nu_1 + \nu_3$) Darling–Dennison resonance region. The i th bands from Table 4 are marked by the capital and small Greek letters. The band number 12 is the spectral component of $^{28}\text{SiH}_4$ with the D_{2d} symmetry, see Table 2 and Figure 2.

spectra regardless of the experimental conditions, which we can not interpret.

DISCUSSION OF THE RESULTS

Fundamental Region. We shall start with the analysis of spectra of $^{28}\text{SiH}_4$ in the fundamental region. Vibrational spectra of SiH_4 in low-temperature matrixes differ significantly from the vibrational spectra in the gas phase and in liquid Ar. For example, in the nitrogen matrix three bands are observed in the region of stretching vibrations and two bands are observed in the region of bending vibrations (Figure 3, Table 3), instead of one rovibrational band in each of the studied spectral regions in the gas phase.³¹ These effects are explained by the change of the symmetry of the SiH_4 molecule caused by an interaction with matrix particles. It is shown¹³ that the SiH_4 molecule with one selected bond (C_{3v} symmetry) is embedded into a cell of a nitrogen matrix without significant cell distortion. Our calculations show that the force constant of one of the four bonds should change by only 1% from the case of the free SiH_4 molecule to provide recorded splitting of the bands (see Table A2 in Appendix A). The same results was obtained for GeH_4 .¹²

The ν_3 (with the F_2 symmetry species) band of SiH_4 molecules active in absorption should split in the N_2 matrixes into two bands A_1 and E with the intensity ratio 1:2. In the gas phase the frequencies of the stretching vibrations $\nu_1(A_1) = 2186.87 \text{ cm}^{-1}$ and $\nu_3(F_2) = 2189.19 \text{ cm}^{-1}$ almost coincide.³¹ The intensity of the $\nu_1(A_1)$ band becomes comparable with the ν_3 intensity due to the resonance interaction of ν_1 level with the A_1 component of the split ν_3 level. From the resonance origin of the triplet with III, IV, and V components (see Figure 3) it follows that $I_V(E) + I_{IV}(A_1) + I_{III}(A_1) = 3(I_{IV}(A_1) + I_{III}(A_1))$, where I_i is the integral intensities.¹²

The ν_4 (F_2) bending band at 913.47 cm^{-1} is also split into two components A_1 and E in the nitrogen matrix; however, the E component cannot resonate with the $\nu_2(E)$ (974.6 cm^{-1}) vibration because of the large difference between the frequencies of the bending vibrations.³¹ For this reason, a doublet of two components I, II with the ratio of integral intensities ($I_I(E)/I_{II}(A_1) = 2$), is observed (see Table 3) in the bending region.

As noted above, two groups of bands of $^{28}\text{SiH}_4$ observed in the argon matrixes vary independently with changes of deposition and annealing temperature. These bands can be assigned to SiH_4 molecules of different symmetry embedded in an argon matrix, in which the molecules occupy the cells with different microenvironment.

The narrow bands (a value of full width at half-maximum (fwhm) = $0.05\text{--}0.15 \text{ cm}^{-1}$), indicated as I, II, III, and IV in Figure 3, can be assigned to the $^{28}\text{SiH}_4$ molecules of the D_{2d} symmetry. Upon lowering the symmetry from T_d to D_{2d} the ν_4 state is split in accordance with the correlation table $F_2 \rightarrow B_2 + E$ (Table A1, Appendix A). In the bending region two strong bands I and II are observed with a splitting 0.35 cm^{-1} and the intensity ratio ($I_I/I_{II} = 2$). The calculation in the harmonic approximation with the force constants of two opposite angles increased by 0.2% leads to splitting values and relative intensities close to the experimental values (Table A3). In the same calculation the splitting value of the ν_3 state is about 0.1 cm^{-1} . High-resolution spectroscopy allowed us to observe a doublet in the ν_3 region with a splitting of $0.15(5) \text{ cm}^{-1}$ (Table 3), which is in agreement with the calculation. The ratio of the intensity of high-frequency component IV of the ν_3 band to the intensity of the low-frequency component III is ($I_{IV}/I_{III} = 0.5$), as well as for bending vibration.

In the Ar matrix a number of blue-shifted bands is always observed (see Table 4). Three bands A, B, and Γ are observed in the ν_4 spectral region and four bands Δ , E, Z, and H are observed in the stretching region. The observed spectrum is interpreted as a spectrum of a SiH_4 molecule distorted to the C_1 symmetry in an Ar matrix. It is reasonable to attribute these spectra, consisting of narrow and broad bands, to silane molecules located at two different sites. The red-shifted narrow lines may be attributed to $\ll\text{matrix isolated}\gg$ silane, since lines of this type are usually observed in matrix-isolation spectra. In the second case, the SiH_4 molecule occupies the so-called a point-defect site in an Ar crystal without significant distortion of the crystal lattice. The site size R is usually possible to estimate using the data on the crystal density $\rho(\text{g/cm}^3)$ at the melting temperature, for face-centered cubic structure $R = (M/(\rho N_A \sqrt{2}))^{1/3}$, where M is molar mass and N_A is Avogadro's number. It follows from estimates that in argon crystal $R = 3.22 \text{ \AA}$,³² the radius of silane is about 3.65 \AA ,³³ and formally the SiH_4 molecule cannot occupy a monosubstitutional site in Ar crystals. However, in reality there is a nonzero probability to put silane molecule in a free space in an argon matrix. In this case, silane is strongly distorted and changes its symmetry from T_d to the low-symmetry C_1 group. The small size of the cell in an argon matrix leads to an increase in the contribution of repulsive forces to the intermolecular interaction potential, and as a result, the SiH_4 band are blue-shifted.³⁴

It should be noted that similar spectra in the ν_3 and ν_4 regions in nitrogen and argon matrixes were obtained earlier, but at a lower resolution of $0.5\text{--}0.1 \text{ cm}^{-1}$.^{24,27} We agree with the conclusions of Wilde et al.²⁴ in which two types of bands (narrow and relatively broad) were attributed to two types of SiH_4 molecules of different structure isolated in an argon matrix. In another work,²⁷ where similar experimental results were obtained in an Ar matrix, a different interpretation of the spectrum was suggested. It was assumed that the blue-shifted A, B, Γ and Δ , E, Z, H bands belong to phonon sidebands arising due to the interaction of the silane vibrations with the matrix lattice vibrations. However, this interpretation is unlikely because the relative intensity of bands in the blue and red spectral regions depends on temperature and cannot be assigned to combination bands.

Region of the Combination Bands. As for the fundamental region the matrix spectra of SiH_4 in the region of combination bands noticeably differ from the spectra in the gas phase and in low temperature solution: instead one or two bands typical of a T_d molecule a number of peaks are observed near combination transition frequencies (Figures 1 and 2). As was mentioned above, the spectra of SiH_4 in nitrogen and argon matrixes are different from each other. As we will show below these features are in good agreement with the assumption that SiH_4 has the C_{3v} symmetry in a N_2 matrix and the D_{2d} symmetry in an Ar matrix.

Some features are common for all the bands that were recorded. In the Ar matrixes in all spectral regions the SiH_4 bands are shifted to lower frequencies, see Figures 1 and 2, while in the N_2 matrixes a blue shift of the bands is constantly observed. Only in the case of the $\nu_2 + \nu_4$ bending combination vibration the frequency of free molecules coincides with the frequency in the N_2 matrix spectrum (Figure 1). A similar picture was observed in the ν_4 fundamental region (see above). The observed values of band splitting due to symmetry reduction in the Ar matrix are an order of magnitude smaller

than distortions of the vibrational spectrum of SiH₄ in a N₂ matrix.

The spectrum bands in Ar matrixes are much narrower than in N₂ matrixes: a fine structure in accordance with the D_{2d} symmetry is observed with confidence only due to low temperature and high resolution of the experiment. Integral band intensities within error limits coincide with the spectrum data of solution of SiH₄ in liquid Ar at T = 96 K,³⁰ see Table 2.

For transitions that include bending vibrations (ν_2 and ν_4), the frequencies of the bands can be estimated as sums of the corresponding fundamental band frequencies. With the anharmonicity correction taken into account, the estimated frequencies are shifted as a whole into the region of experimental bands. These frequencies are marked by vertical lines under the spectra in Figure 1. To describe the bands in the ($2\nu_3, \nu_1 + \nu_3$) region, the local mode approach can be used. It was successfully applied to the description of frequencies of transition to high (up to the eighth order) stretching vibrational states of the T_d-symmetry SiH₄ and GeH₄ molecules.³⁵ It allows calculation of the relative intensities of the band along with the frequencies. The results of these calculations are presented in Figure 2 as stick spectra: the sticks are located at the calculated frequencies and the height of the sticks is proportional to the calculated intensity value.

Table A4 in Appendix A is useful to determine how many bands one can observe in the specific region for molecules of different symmetry. In most cases only one transition is active in the specific combination region in IR spectra of molecules with the T_d symmetry (SiH₄ in the gas phase), but for molecules with the D_{2d} and C_{3v} symmetry a number of bands is allowed. Their intensities can be low especially for bands arisen from forbidden transitions for molecules with the T_d symmetry because of the small perturbations. Such bands may not be observed in the experimental spectra.

The ($\nu_2 + \nu_4$) Spectral Region. The spectra in this region are presented in the upper panel of Figure 1. In the spectra in both matrixes the bands corresponding to transitions to $\nu_2 + \nu_k$ combination states have a large value of fwhm. Table 1 shows the frequency of the band obtained as a result of averaging of eight spectra at the same temperature. One can suppose that the ν_2 vibration has a strong interaction with the matrix. In the C_{3v} symmetry group the ν_2 vibration does not split; we will denote it as $\nu_{N_2}^{VI}$. The intensity of this band is very low since it is forbidden in the T_d symmetry group. According to our calculation, the intensity is lower than 1000th of the ν_3 band intensity (see Table A3 in Appendix A). This band was not observed in our spectra. According to representation correlation $E \rightarrow (A_1 + B_1)$, in the D_{2d} symmetry group there are two bands in the ν_2 region (see Table A1). Below they are denoted as $\nu_{Ar}^V(B_1)$ and $\nu_{Ar}^{VI}(A_1)$. Both bands are inactive in IR absorption and have not been detected in our experiment. According to our calculation, $\nu_{Ar}^{VI}(A_1) - \nu_{Ar}^V(B_1) = 0.5 \text{ cm}^{-1}$ (Table A3). Interpretation of all $\nu_2 + \nu_k$ bands was based on the facts mentioned above.

In the N₂ matrix spectrum two bands are observed; the distance between them is 4.4 cm⁻¹, which is close to the splitting in the fundamental region of ν_4 (3.2 cm⁻¹). Strong band 1 corresponds to a transition to the F₂ → (A₁ + E) split state, its components are not resolved because the bands are broad, like all bands corresponding to transitions to $\nu_2 + \nu_k$ states. This band is combination $\nu_{N_2}^I(A_1 + E) = \nu_{N_2}^I(E) + \nu_{N_2}^{VI}(E)$, where the superscript index is the number of the band introduced in Figures 1 and 3 and in Tables 1 and 3, and the

$\nu_{N_2}^{VI}(E)$ band was denoted above. Band 2 is weak and corresponds to a transition to the E state arisen from splitting of the F₁ state, transition to which is inactive in the T_d group: $\nu_{N_2}^2(E) = \nu_{N_2}^{II}(A_1) + \nu_{N_2}^{VI}(E)$.

In the Ar matrix spectrum three active bands are observed, which is in good agreement with the representation correlation (Table A4). Broader bands 1 and 2 are combinations $\nu_{Ar}^I(E) = \nu_{Ar}^I(E) + \nu_{Ar}^V(B_1)$ and $\nu_{Ar}^2(E) = \nu_{Ar}^I(E) + \nu_{Ar}^{VI}(A_1)$. The superscript indexes match the band numbers in Figures 2 and 3 and in Tables 2 and 3 except the indexes V and VI, which were introduced above. Band 3 corresponds to the combination $\nu_{Ar}^3(B_2) = \nu_{Ar}^{II}(B_2) + \nu_{Ar}^{VI}(A_1)$. The band is considerably narrower than those two having the symmetry species E. It is evident that the A₁ sublevel of the ν_2 vibration is less broadened than the E sublevel of this vibration.

The ($\nu_3 + \nu_4, \nu_1 + \nu_4$) Spectral Region. The spectra in this region are presented in the middle panel of Figure 1. Unlike purely stretching vibrations, the $\nu_1 \approx \nu_3$ resonance in this spectral region is relatively weak. The squares of mixing coefficients of wave functions in the normal coordinate basis calculated with the use of "ab initio" force field parameters for $\nu_1 + \nu_4 \approx \nu_3 + \nu_4$ states make 83.7% and 14.2%, the corresponding values for $\nu_1 + \nu_3 \approx 2\nu_3$ state are 51.2% and 47.7%.³⁶ For this reason the distances between $\nu_3 + \nu_4$ and $\nu_1 + \nu_4$ combination bands are relatively small in comparison with the situation in the ($2\nu_3, \nu_1 + \nu_3$) region. However, the resonance makes the interpretation not so clear.

In the spectrum of a molecule with the C_{3v} symmetry (N₂ matrix) seven bands should be observed in the ($\nu_1 + \nu_4, \nu_3 + \nu_4$) region. In fact, only four bands are observed in the spectrum unambiguously. Band 3 is the combination $\nu_{N_2}^3(E) = \nu_{N_2}^I(E) + \nu_{N_2}^{III}(A_1)$. The highest-frequency band 6 corresponds to the transition to $\nu_{N_2}^6(E) = \nu_{N_2}^{II}(A_1) + \nu_{N_2}^V(E)$ state. The $\nu_{N_2}^4(A_1 + E) = \nu_{N_2}^I(E) + \nu_{N_2}^V(E)$ band consists of two unresolved bands with species A₁ and E. The last band in this region is $\nu_{N_2}^5(A_1) = \nu_{N_2}^I(E) + \nu_{N_2}^V(E)$.

While in the spectrum of solution in liquid Ar at a frequency of 3089 cm⁻¹ one can observe a band with fwhm = 16 cm⁻¹, interpreted in work³⁰ as a transition to the ($\nu_3 + \nu_4$) combined state, one can find five bands in the Ar matrix spectrum. Two groups of bands at a distance of about 4 cm⁻¹ are observed, their presence being explained as follows: the $\nu_{Ar}^4(E) = \nu_{Ar}^I(E) + \nu_1(A_1)$ and $\nu_{Ar}^5(B_2) = \nu_{Ar}^{II}(B_2) + \nu_1(A_1)$ bands from the low frequency group belong to the sums of two split ν_4 band components and the ν_1 band forbidden in absorption; the bands in the high frequency group are combinations with the ν_4 band components $\nu_{Ar}^6(B_2) = \nu_{Ar}^I(E) + \nu_{Ar}^{III}(E)$, $\nu_{Ar}^7(E) = \nu_{Ar}^I(E) + \nu_{Ar}^{IV}(B_2)$, and $\nu_{Ar}^8(E) = \nu_{Ar}^{II}(B_2) + \nu_{Ar}^{III}(E)$.

The ($\nu_2 + \nu_3$) Spectral Region. The spectra are shown in the bottom panel of Figure 1. In the N₂ matrix spectrum three bands are observed instead of predicted four: (A₁ + E), E, E. All these bands are broadened because, as noted above, all transitions to $\nu_2 + \nu_k$ combination states have a large value of fwhm. Bands 7 and 8 are the combinations $\nu_{N_2}^7(E) = \nu_{N_2}^{III}(A_1) + \nu_{N_2}^{VI}(E)$ and $\nu_{N_2}^8(E) = \nu_{N_2}^{IV}(A_1) + \nu_{N_2}^{VI}(E)$, respectively. Band 9 consists of two unresolved bands $\nu_{N_2}^9(A_1 + E) = \nu_{N_2}^V(E) + \nu_{N_2}^{VI}(E)$ with the symmetry species A₁ and E.

In the Ar matrix spectrum two relatively broad bands are observed instead of three predicted (Table A4). This is explained by the fact that the splitting of the ($\nu_2 + \nu_3$) band is only determined by the ν_2 state splitting, the ν_3 band splitting being very small. Band 9 is the combination $\nu_{Ar}^9(E) = \nu_{Ar}^{III}(E) + \nu_{Ar}^V(B_1)$. Band 10 is the superposition of two bands $\nu_{Ar}^{10}(E) =$

$\nu_{\text{Ar}}^{\text{III}}(E) + \nu_{\text{Ar}}^{\text{VI}}(A_1)$ and $\nu_{\text{Ar}}^{10}(B_2) = \nu_{\text{Ar}}^{\text{IV}}(B_2) + \nu_{\text{Ar}}^{\text{VI}}(A_1)$ unresolved in the experimental spectra.

The $(2\nu_3, \nu_1 + \nu_3)$ Spectral Region. In this region a strong Darling–Dennison resonance is observed in the gas phase spectra and there are two resonance components with essentially different intensities. The value of resonance splitting is about of $\sim 70 \text{ cm}^{-1}$. The same picture is present in matrix spectra. For convenience, these spectra have been divided into two parts: low frequency (\mathcal{LF}) and high frequency (\mathcal{HF}) parts, which are displayed in Figure 2.

As was mentioned above the experimental frequencies and intensities of the bands in the $(2\nu_3, \nu_1 + \nu_3)$ region can be described well by the local mode model. The applicability of this model in the transition from the gas phase to the inert solutions was discussed earlier.³⁴ The parameters can be obtained from the gas phase spectra, where the frequencies of the band are well-known (see Supporting Information). Within the framework of the local mode model a T_d symmetry molecule with X–H bonds can be represented as four partial anharmonic oscillators, weakly coupled to one another. The dipole moment function of this molecule describing stretching vibration intensity in the fundamental and overtone transition regions can be written as follows:

$$\vec{P} = \sum_{i=1}^4 P_i \vec{e}_i + \sum_{\substack{i,j=1 \\ i \neq j}}^4 P_{ij} \vec{e}_{ij} \quad (1)$$

$$P_i = P_0 + P'_i r_i + \frac{1}{2} P''_i r_i^2$$

$$P_{ij} = P''_{ij} r_i r_j$$

where \vec{e}_i is the unit vector along an i th bond, \vec{e}_{ij} is the unit vector along the bisector of the angle between bonds i and j , and r_i is the displacement coordinate. The vibrational transition moments in \mathcal{HF} part are mainly determined by the second derivative of the dipole moment function P_{ij} and is naturally smaller than the moment of low frequency transition. Indeed, the vibrational spectrum of a SiH_4 molecule has a much more intense low-frequency overtone band than a high-frequency one, for example, in the spectrum of solution in liquid argon.³⁰ The same picture, corresponding to a T_d symmetry molecule, is observed in the SiH_4 spectrum in an Ar matrix (Table 2 and

Figure 2). The Ar matrix spectrum in this spectral region confirms the conclusion that the stretching vibrations are weakly perturbed in the matrix conditions. The splitting due to the D_{2d} symmetry should be smaller than the experimental widths of the bands observed in this region.

The N_2 matrix shows another picture: when embedded in an N_2 crystal cell, the SiH_4 molecule distorts, and its symmetry reduces to C_{3v} .^{12,13} Selecting one of SiH bonds (C_3 axis) causes a large splitting of bands both in the stretching and bending fundamental regions. Using these experimental data and the local mode model, one can calculate the vibrational spectrum in the $(2\nu_3, \nu_1 + \nu_3)$ region.

The decrease in the symmetry from T_d to C_{3v} in the N_2 matrix is modeled by changing the frequency of one (the first) of the partial oscillators $\nu_1 = \nu_0 - \Delta$, matrix elements of partial oscillator interaction being considered equal to those calculated from the gas spectrum (see Supporting Information). The characteristic of the selected partial oscillator Δ can be estimated from a harmonic field describing experimental frequencies and absorption band intensities in the fundamental spectrum region of a SiH_4 molecule in the N_2 matrix (Appendix A):

$$\Delta = \frac{1}{2} \nu_0 \frac{\Delta K_{rr}}{K_{rr}} = 7 \text{ cm}^{-1}$$

where $(\Delta K_{rr}/K_{rr}) = 0.0065$, $\nu_0 = 2206.4 \text{ cm}^{-1}$.

The absorption band frequencies and intensities in the overtone spectrum region are obtained by solving two secular equations separately (see Supporting Information). Considering this, let us restrict ourselves to determining relative intensities within each overtone zone. In the adopted approximation the dipole moment function (eq 1) corresponds to a T_d symmetry molecule (zero-order approximation). The matrix elements of dipole moment of each partial oscillator are projected on the X , Y , and Z axes of the laboratory system and multiplied by their eigenvector of the corresponding secular equation. The relative absorption band intensities are determined by the sum of squares of projections $(P_X)^2 + (P_Y)^2 + (P_Z)^2$.

The secular equation for the overtone-region low-frequency zone has the form:

$$\begin{vmatrix} \langle 2000 | & 2\nu_0 - 2\Delta + 2x - \lambda & W_2^I & W_2^I & W_2^I \\ \langle 0200 | & W_2^I & 2\nu_0 + 2x - \lambda & W_2^I & W_2^I \\ \langle 0020 | & W_2^I & W_2^I & 2\nu_0 + 2x - \lambda & W_2^I \\ \langle 0002 | & W_2^I & W_2^I & W_2^I & 2\nu_0 + 2x - \lambda \end{vmatrix} = 0$$

The value of interaction matrix element $W_2^I = -0.12 \text{ cm}^{-1}$ was obtained in Supporting Information. In our case the value of resonance detuning is much larger than the interaction matrix element: $2\Delta = 14 \gg 0.12 \text{ cm}^{-1}$, which almost prevents an oscillator with frequency $2\nu_0 - 2\Delta + 2x$ from interacting with the other three. It has the A_1 symmetry species, and its band intensity is equal to 0.25 of the whole intensity in the zone. The other three oscillators with frequencies $2\nu_0 + 2x$ yield

two bands of species A_1 and E , their splitting equal to $3W_2^I$ (Figure 2, \mathcal{LF}). As a result, all the calculated frequencies and relative band intensities of the low-frequency zone, compared to the experiment, are presented in Figure 2, \mathcal{LF} .

The secular equation for the overtone-region high-frequency zone is as follows:

$$\begin{array}{c|cccccc}
 \langle 1100 | & 2\nu_0 - \Delta - \lambda & W_2^{II} & W_2^{II} & W_2^{II} & W_2^{II} & 0 \\
 \langle 1010 | & W_2^{II} & 2\nu_0 - \Delta - \lambda & W_2^{II} & W_2^{II} & 0 & W_2^{II} \\
 \langle 1001 | & W_2^{II} & W_2^{II} & 2\nu_0 - \Delta - \lambda & 0 & W_2^{II} & W_2^{II} \\
 \langle 0110 | & W_2^{II} & W_2^{II} & 0 & 2\nu_0 - \lambda & W_2^{II} & W_2^{II} \\
 \langle 0101 | & W_2^{II} & 0 & W_2^{II} & W_2^{II} & 2\nu_0 - \lambda & W_2^{II} \\
 \langle 0011 | & 0 & W_2^{II} & W_2^{II} & W_2^{II} & W_2^{II} & 2\nu_0 - \lambda
 \end{array} = 0$$

where interaction matrix element $W_2^{II} = -0.95 \text{ cm}^{-1}$ was obtained in [Supporting Information](#). By solving the secular equation we obtain two A_1 levels and two E ones. The result of the solution with relative intensities is shown in [Figure 2](#), \mathcal{HF} .

Thus, the result of the calculation of the spectrum in the overtone region of stretching vibrations of $^{28}\text{SiH}_4$ molecule in the nitrogen matrix confirms the reduction of molecule symmetry to C_{3v} . When a molecule is embedded into the nitrogen matrix defect, an indispensable frequency difference of one of partial oscillators is observed.¹³ The equivalence of the other three partial oscillators is demonstrated by the calculation with the help of local mode model.

Overtone of a C_1 -Symmetry $^{28}\text{SiH}_4$ Molecule in the Argon Matrix. The spectra of overtones of SiH_4 molecule deformed to C_1 symmetry were recorded in $2\nu_3$ region. These bands are presented in the bottom panel of [Figure 4](#). Unlike the situation in the fundamental region, the bands have equal intensities (within limits of a relatively large error) due to a small value of the matrix element of interaction of partial oscillators $W_2^I = -0.12 \text{ cm}^{-1}$ ([Supporting Information](#)). In the fundamental region the radically different relative intensities and half-widths of the four «broad» bands can be explained by close values of the splitting and perturbation matrix element ([Supporting Information](#))

CONCLUSIONS

The results of the present study have demonstrated the efficiency of analysis of the spectra in the overtone region for describing of possible changes in the symmetry of high-symmetry molecules in low-temperature matrixes. High-resolution spectroscopy is a very useful tool for recording the band splitting and for analyzing the spectra. In general, the observed change in the symmetry of the XH_4 molecule and a radical change in its spectrum are determined only by a slight change in the force constants of these molecules.

In this article the absorption spectra of monoisotopic $^{28}\text{SiH}_4$ in the argon and nitrogen matrixes were recorded in the fundamental and combination regions with a resolution of $0.01\text{--}0.1 \text{ cm}^{-1}$ at temperature $T = 6.5\text{--}20 \text{ K}$. The frequencies of observed bands and relative intensities of the second-order transitions were determined. The matrix spectra differ significantly from the vibrational spectra of free SiH_4 : the new vibrational bands were observed both in fundamental and combination regions. The analysis showed that these changes are results of symmetry changing of SiH_4 molecule due to weak interaction with a matrix environment.

In the N_2 matrix SiH_4 molecules undergo a relatively strong perturbation: the bands of only one type of SiH_4 molecules were observed. The symmetry of these molecules reduces to C_{3v} , that is confirmed by spectra in the fundamental and

combination regions. The bands in all the regions are blue-shifted relative to vibrational frequencies of SiH_4 in the gas phase. As was shown previously, the SiH_4 molecules occupy the vacant places in the nitrogen virtually undistorted crystal lattice. Using the local mode model allows satisfactory description of a complex spectrum (frequencies and intensities of the bands) in the overtone region of stretching vibrations.

It was shown that there are at least two types of SiH_4 molecules in the Ar matrix. The molecules with the D_{2d} symmetry are characterized by narrow band doublets with a 0.35 cm^{-1} splitting in the bending region and a 0.1 cm^{-1} splitting in the fundamental region. The combination region spectrum confirms this interpretation: the splitting is maximal for purely bending combined bands, while no splitting is observed in the overtone region of stretching vibrations ($2\nu_3, \nu_1 + \nu_3$). All the bands in the fundamental and combination regions are red-shifted relative to the vibrational frequencies of silane in the gas phase. This type can be considered as “matrix isolated” molecules. The second type of molecules have broader blue-shifted bands and have a low molecular symmetry, presumably C_1 . These molecules are embedded in the argon crystal lattice without its significant distortion.

It should be noted that symmetry changes in low-temperature matrixes can be spectroscopically observed not only for XH_4 molecules but also for other molecules that have degenerated states and XH bond. It gives a possibility for studying of different symmetry types of chemically the same molecule by changing the environment only. However, the well-defined values of band splitting can characterize accurately the interaction of a molecule with a matrix environment and can be a good guide in testing of the models describing such an interaction.

APPENDIX A

The SiH_4 molecule has a tetrahedral symmetry (T_d group). According to the symmetry (see [Table A1](#)), only ν_3 and ν_4 vibrations are active in absorption. To learn how the vibrational

Table A1. Correlation Table for the Species of the T_d Group and Its D_{2d} and C_{3v} Subgroups^a

| T_d | C_{3v} | D_{2d} |
|-------|-----------|-------------|
| A_1 | A_1 | A_1 |
| A_2 | A_2 | B_1 |
| E | E | $A_1 + B_1$ |
| F_1 | $A_2 + E$ | $A_2 + E$ |
| F_2 | $A_1 + E$ | $B_2 + E$ |

^aThe species F_2 are only active in dipole absorption for T_d group; B_2 and E are active for D_{2d} ; and A_1 and E are active for C_{3v} .

spectrum is changed due to the distortion of molecules in matrixes, one should use the correlation of vibrational representations.

After the SiH₄ molecule is deformed to the D_{2d} symmetry, the ν_1 band is still forbidden in absorption. The transition to the ν_2 split vibrational state is also forbidden. In the ν_3 and ν_4 spectral regions doublets with components B₂ and E active in IR spectra should be recorded. The E components should be twice as intense as B₂ components. All the above is observed in the spectra of SiH₄ in argon matrixes. If the molecule is deformed to C_{3v} symmetry, the ν_3 and ν_4 bands split into doublets, and the ν_1 and ν_2 vibrations become active in the IR absorption according to their symmetry. However, because the magnitude of perturbation is small, the band intensity of ν_2 vibration should be very low. The ν_1 frequency is very close to the ν_3 frequency in the ²⁸SiH₄ molecule, which leads to essential intensity borrowing from ν_3 to ν_1 . As a result, a triplet should occur in the ν_3 spectral region. All the above is observed in the spectra of SiH₄ in nitrogen matrixes.

The force field can be presented as coefficients K of quadratic form in natural coordinates. The ²⁸SiH₄ molecule in the gas phase has four vibrations:³¹ ν_1 (A₁) = 2186.87 cm⁻¹, ν_2 (E) = 970.93 cm⁻¹, ν_3 (F₂) = 2189.19 cm⁻¹, and ν_4 (F₂) = 913.47 cm⁻¹. The force field for molecules with the T_d symmetry presented in Table A2 describes these frequencies within 0.1 cm⁻¹ accuracy.

Table A2. Force Fields (cm⁻² × 10⁻⁶) for Different Symmetry Groups That Describe the Fundamental Frequencies of ²⁸SiH₄ Molecules with the T_d Symmetry in the Gas Phase and the Frequency Splitting in the Matrix Spectra of ²⁸SiH₄ With the C_{3v} and D_{2d} Symmetries

| symmetry | K _{rr} | K _{rr'} | K _{rpp} | K _{ppp} | K _{ppp'} |
|------------------------------|-----------------|------------------|------------------|------------------|-------------------|
| T _d | 4.640 | 0.0474 | 0.17 | 0.3938 | 0.0398 |
| C _{3v} ^a | 4.610 | 0.0444 | 0.15 | 0.3938 | 0.0398 |
| D _{2d} ^b | 4.640 | 0.0474 | 0.17 | 0.3943/0.3933 | 0.0398 |

^aFor the C_{3v} symmetry, the force constants of a selected bond are presented. The other constants are the same as for the T_d symmetry.

^bFor the D_{2d} symmetry, the force field coincides with the T_d field except for two constants K_{ppp} for two pairs of opposite angles.

If the diagonal force constant for one bond is changed by 0.03 × 10⁻⁶ cm⁻² (1%) or the interaction constant of this bond with adjacent angles is changed by 0.02 × 10⁻⁶ cm⁻² in the C_{3v} case, the calculated splitting and relative intensities of components are comparable with the values observed in the nitrogen matrix spectra, see Table A3.

Table A3. Experimental and Calculated Splitting Values $\delta\nu$ (Measured from the Frequency of the Strongest Band) and Relative Intensities $I_{rel} = (1000I/I_3)$ of Fundamental Bands in Absorption Spectra of ²⁸SiH₄ with the D_{2d} and C_{3v} Symmetry

| region | species | C _{3v} | | | | D _{2d} | | | | |
|----------------|----------------|-----------------------------|-------|-----------|-------|-----------------------------|-------|-----------|-------|-----|
| | | $\delta\nu, \text{cm}^{-1}$ | | I_{rel} | | $\delta\nu, \text{cm}^{-1}$ | | I_{rel} | | |
| | | exptl | calcd | exptl | calcd | exptl | calcd | exptl | calcd | |
| ν_1, ν_3 | E | 0 | 0 | 655 | 670 | E | 0 | 0 | 670 | 670 |
| | A ₁ | -3.4 | -3.1 | 245 | 210 | B ₂ | -0.16 | <0.1 | 340 | 330 |
| | A ₁ | -10.07 | -9.5 | 100 | 120 | A ₁ | -2.8 | 0 | 0 | 0 |
| ν_2 | E | | 0 | | <1 | B ₁ | | 0 | | 0 |
| | | | | | | A ₁ | | +0.5 | | 0 |
| ν_4 | E | 0 | 0 | 910 | 890 | E | 0 | 0 | 700 | 890 |
| | A ₁ | +2.91 | +2.6 | 490 | 450 | B ₂ | +0.33 | +0.6 | 300 | 450 |

The splitting in the spectra of SiH₄ in the argon matrix is small. For a D_{2d} molecule, the 0.1% change of force constants of opposite angles leads to splitting values comparable with the experimental data (Table A3).

Table A4 summarizes the symmetry species of the bands in various combination band regions of the SiH₄ molecule

Table A4. Symmetry Species of Overtone and Combinational Bands on Passing from the T_d Symmetry Group to C_{3v} and D_{2d}; the Number of IR Active States Is Shown in Parentheses

| region | T _d | C _{3v} | D _{2d} |
|-----------------|--|---|---|
| $\nu_2 + \nu_4$ | F ₁ + F ₂ (1) | A ₁ + A ₂ + 2E (3) | A ₂ + B ₂ + 2E (3) |
| $\nu_3 + \nu_4$ | A ₁ + E + F ₁ + F ₂ (1) | 2A ₁ + A ₂ + 3E (5) | 2A ₁ + A ₂ + B ₁ + B ₂ + 2E (3) |
| $\nu_1 + \nu_4$ | F ₂ (1) | A ₁ + E (2) | B ₂ + E (2) |
| $\nu_2 + \nu_3$ | F ₁ + F ₂ (1) | A ₁ + A ₂ + 2E (3) | A ₂ + B ₂ + 2E (3) |
| 2 ν_3 | A ₁ + E + F ₂ (1) | 2A ₁ + 2E (4) | 2A ₁ + B ₁ + B ₂ + E (2) |
| $\nu_1 + \nu_3$ | F ₂ (1) | A ₁ + E (2) | B ₂ + E (2) |
| $\nu_1 + \nu_2$ | E (0) | E (1) | A ₁ + B ₁ (0) |

deformed to different symmetries. The species for the T_d group were obtained as direct product of representations of corresponding fundamental vibrations (for example, see monograph³⁷). The species for the C_{3v} and D_{2d} groups were obtained using the Table A1. The number of IR active states based on the selection rules (see Title of Table A1) is presented in parentheses.

■ ASSOCIATED CONTENT

📄 Supporting Information

The Supporting Information is available free of charge on the ACS Publications website at DOI: 10.1021/acs.jpca.7b02798.

Computation of frequencies in the fundamental and ($\nu_1 + \nu_3$, 2 ν_3) regions of the SiH₄ molecule in the gas phase using local mode model. The estimation of parameters that was used in calculation of frequencies and intensities of SiH₄ in the N₂ matrix (PDF)

■ AUTHOR INFORMATION

Corresponding Author

*Tel: +7(812) 428 74 19. E-mail: k.tokhadze@spbu.ru.

ORCID

Ruslan E. Asfin: 0000-0002-5886-101X

Konstantin G. Tokhadze: 0000-0003-1131-8535

Notes

The authors declare no competing financial interest.

ACKNOWLEDGMENTS

This work was supported by the Russian Foundation for Basic Research (grant no. 15-03-04605). The spectra were recorded in the Center for Geo-Environmental Research and Modeling (GEOMODEL) of Research Park of St. Petersburg State University.

REFERENCES

- (1) *Vibrational Spectroscopy of Trapped Species: Infrared and Raman Studies of Matrix-Isolated Molecules, Radicals and Ions*; Hallam, H. E., Ed.; John Wiley & Sons: London, 1973.
- (2) *Matrix Isolation Spectroscopy*; Barnes, A. J., Orville-Thomas, W. J., Müller, A., Gaufrès, R., Eds.; Springer: Dordrecht, Netherlands, 1981.
- (3) *Chemistry and Physics of Matrix-Isolated Species*; Andrews, L., Moskovits, M., Eds.; Elsevier Science Publishers: Amsterdam, 1989.
- (4) Knözinger, E.; Babka, E.; Hallamasek, D. Cage Structure and Long-Range Order in Solid Rare Gas Matrixes: A Combined FTIR and XRD Study. *J. Phys. Chem. A* **2001**, *105*, 8176–8182.
- (5) Kolomiitsova, T. D.; Mielke, Z.; Shchepkin, D. N.; Tokhadze, K. G. Infrared Matrix Isolation Spectra of SF₆ Dimers. *Chem. Phys. Lett.* **2002**, *357*, 181–188.
- (6) Tokhadze, I. K.; Kolomiitsova, T. D.; Tokhadze, K. G.; Shchepkin, D. N. The Effect of Resonance Interactions on the Absorption Spectra of (SF₆)₂ Dimers in Low-Temperature matrixes: Calculations and Experiment. *Opt. Spectrosc.* **2007**, *102*, 396–407.
- (7) Tokhadze, I. K.; Kolomiitsova, T. D.; Shchepkin, D. N.; Tokhadze, K. G.; Mielke, Z. Influence of Resonance Interactions and Matrix Environment on the Spectra of SF₆ Dimers in Low-Temperature Nitrogen Matrixes. Theory and Experiment. *J. Phys. Chem. A* **2009**, *113*, 6334–6341.
- (8) Tokhadze, I. K.; Kolomiitsova, T. D.; Tokhadze, K. G.; Shchepkin, D. N. Structures of Vibrational Absorption Bands of the SiF₄ Molecule in a Low-Temperature Nitrogen Matrix. *Opt. Spectrosc.* **2014**, *117*, 525–533.
- (9) Ignatov, S. K.; Kolomiitsova, T. D.; Mielke, Z.; Razuvaev, A. G.; Shchepkin, D. N.; Tokhadze, K. G. A Matrix Isolation and Theoretical Study of SiF₄ Dimers Spectra. *Chem. Phys.* **2006**, *324*, 753–766.
- (10) Paulson, S. L.; Barnes, A. J. Trihalogenomethane - Base Complexes Studied by Vibrational Spectroscopy in Low-Temperature matrixes. *J. Mol. Struct.* **1982**, *80*, 151–158.
- (11) Asfin, R. E.; Melikova, S. M.; Domanskaya, A. V.; Rodziewicz, P.; Rutkowski, K. S. Degeneracy Lifting Effect in the FTIR Spectrum of Fluoroform Trapped in a Nitrogen Matrix. An Experimental and Car–Parrinello Molecular Dynamics Study. *J. Phys. Chem. A* **2016**, *120*, 3497–3503.
- (12) Kolomiitsova, T. D.; Savvateev, K. F.; Tokhadze, K. G.; Shchepkin, D. N.; Sennikov, P. G.; Vel'muzhova, I. A.; Bulanov, A. D. Vibrational Spectra of Monoisotopic SiH₄ and GeH₄ in Low-Temperature matrixes. *Opt. Spectrosc.* **2012**, *112*, 563–573.
- (13) Kolomiitsova, T. D.; Savvateev, K. F.; Shchepkin, D. N.; Tokhadze, I. K.; Tokhadze, K. G. Infrared Spectra and Structures of SiH₄ and GeH₄ Dimers in Low-Temperature Nitrogen Matrixes. *J. Phys. Chem. A* **2015**, *119*, 2553–2561.
- (14) Lundell, J.; Pettersson, M.; Khriachtchev, L.; Rasanen, M.; Chaban, G. M.; Gerber, R. B. Infrared Spectrum of HXeI Revisited: Anharmonic Vibrational Calculations and Matrix Isolation Experiments. *Chem. Phys. Lett.* **2000**, *322*, 389–394.
- (15) Lapiński, A.; Spanget-Larsen, J.; Waluk, J.; Radziszewski, J. G. Vibrations of Nitrous Oxide: Matrix Isolation Fourier Transform Infrared Spectroscopy of Twelve N₂O Isotopomers. *J. Chem. Phys.* **2001**, *115*, 1757–1764.
- (16) Fajardo, M. E.; Tam, S.; DeRose, M. E. Matrix Isolation Spectroscopy of H₂O, D₂O, and HDO in Solid Parahydrogen. *J. Mol. Struct.* **2004**, *695*, 111–127.
- (17) Himmel, H. J.; Gaertner, B. Characterization of Isolated Ga₂ Molecules by Resonance Raman Spectroscopy and Variations of Ga-Ga Bonding. *Chem. - Eur. J.* **2004**, *10*, 5936–5941.
- (18) Akai, N.; Katsumoto, Y.; Ohno, K.; Aida, M. Vibrational Anharmonicity of Acetic Acid Studied by Matrix-Isolation near-Infrared Spectroscopy and DFT Calculation. *Chem. Phys. Lett.* **2005**, *413*, 367–372.
- (19) Perchard, J. P.; Romain, F.; Bouteiller, Y. Determination of Vibrational Parameters of Methanol from Matrix-Isolation Infrared Spectroscopy and Ab Initio Calculations. Part 1 - Spectral Analysis in the Domain 11000–200 cm⁻¹. *Chem. Phys.* **2008**, *343*, 35–46.
- (20) Wan, L.; Wu, L.; Liu, A. W.; Hu, S. M. Neon Matrix Isolation Spectroscopy of CO₂ Isotopologues. *J. Mol. Spectrosc.* **2009**, *257*, 217–219.
- (21) Marushkevich, K.; Khriachtchev, L.; Lundell, J.; Domanskaya, A. V.; Rasanen, M. Vibrational Spectroscopy of Trans and Cis Deuterated Formic Acid (HCOOD): Anharmonic Calculations and Experiments in Argon and Neon matrixes. *J. Mol. Spectrosc.* **2010**, *259*, 105–110.
- (22) Olbert-Majkut, A.; Ahokas, J.; Lundell, J.; Pettersson, M. Raman Spectroscopy of Formic Acid and Its Dimers Isolated in Low Temperature Argon matrixes. *Chem. Phys. Lett.* **2009**, *468*, 176–183.
- (23) Olbert-Majkut, A.; Ahokas, J.; Lundell, J.; Pettersson, M. Raman Spectroscopy of Acetic Acid Monomer and Dimers Isolated in Solid Argon. *J. Raman Spectrosc.* **2011**, *42*, 1670–1681.
- (24) Wilde, R. E.; Srinivasan, T. K. K.; Harral, R. W.; Sankar, S. G. Matrix-Isolated Silane. Infrared Spectra. *J. Chem. Phys.* **1971**, *55*, 5681–5692.
- (25) Abouafmarguin, L.; Lloret, A. Silane Glow-Discharge - Trapping of the Free-Radicals in Solid Argon. *J. Non-Cryst. Solids* **1985**, *77-78*, 761–764.
- (26) Lloret, A.; Abouafmarguin, L. IR Detection by Matrix-Isolation Technique of Radicals Produced in a Silane Discharge. *Chem. Phys.* **1986**, *107*, 139–143.
- (27) Li, L.; Graham, J. T.; Weltner, W. Infrared Spectra of Silane in Solid Argon and Hydrogen. *J. Phys. Chem. A* **2001**, *105*, 11018–11025.
- (28) Cabana, A.; Savitsky, G. B.; Hornig, D. F. Vibration—Rotation Spectra of CH₄ and CD₄ Impurities in Xenon, Krypton, and Argon Crystals. *J. Chem. Phys.* **1963**, *39*, 2942–2950.
- (29) Jones, L. H.; Ekberg, S. A.; Swanson, B. I. Hindered Rotation and Site Structure of Methane Trapped in Rare Gas Solids. *J. Chem. Phys.* **1986**, *85*, 3203–3210.
- (30) Sennikov, P. G.; Shkrugin, V. E.; Melikova, S. M.; Lebedeva, Y. A. Vibrational Spectra of Solution of Highly Pure Silane and Germane in Liquid Argon. *Vysok. veshchestva (High purity Compd.) (Russian)* **1992**, *6*, 127–133.
- (31) Owens, A.; Yurchenko, S. N.; Yachmenev, A.; Thiel, W. A Global Potential Energy Surface and Dipole Moment Surface for Silane. *J. Chem. Phys.* **2015**, *143*, 244317.
- (32) *Cryocrystals*; Verkin, B. I., Prikhot'ko, A. F., Eds.; Naukova Dumka: Kyiv, 1983.
- (33) Klein, M. L.; Morrison, J. A.; Weir, R. D. Molecular Motions in Solid Isotopic Silanes. *Discuss. Faraday Soc.* **1969**, *48*, 93–101.
- (34) Kolomiitsova, T. D.; Shchepkin, D. N. Vibrational Spectra of Polyatomic Molecules. In *Molecular Cryospectroscopy*; Clark, R. J. H., Hester, R. E., Eds.; John Wiley & Sons: Chichester, 1995; pp 92–134.
- (35) Permogorov, D.; Campargue, A. The Local Mode Model in Silanes and Germanes. *Mol. Phys.* **1997**, *92*, 117–125.
- (36) Wang, X.-G.; Sibert, E. L., III A Nine-Dimensional High Order Perturbative Study of the Vibration of Silane and Its Isotopomers. *J. Chem. Phys.* **2000**, *113*, 5384.
- (37) Wilson, E. B.; Decius, J. C.; Cross, P. C. *Molecular Vibrations. The Theory of Infrared and Raman Vibrational Spectra*; McGraw-Hill Book Company Inc.: New York, 1955.